



# Subseasonal-to-Seasonal Predictability Assessment of an Early Heat Wave in the Eastern Mediterranean in May 2020<sup>†</sup>

Dimitris Mitropoulos<sup>1,\*</sup>, Ioannis Pytharoulis<sup>1,2</sup>, Prodromos Zanis<sup>1,2</sup> and Christina Anagnostopoulou<sup>1</sup>

<sup>1</sup> Department of Meteorology and Climatology, School of Geology, Aristotle University of Thessaloniki, 54124 Thessaloniki, Greece

<sup>2</sup> Center for Interdisciplinary Research and Innovation (CIRI\_AUTH), Balkan Center, Buildings A & B, Thessaloniki-Thermi Rd., 57001 Thessaloniki, Greece

\* Correspondence: dimitrism@geo.auth.gr

<sup>†</sup> Presented at the 16th International Conference on Meteorology, Climatology and Atmospheric Physics—COMECAP 2023, Athens, Greece, 25–29 September 2023.

**Abstract:** Greece experienced an unusual heat wave in mid-May 2020, since it was observed earlier than the common Mediterranean heat wave period. On May 16th, the maximum air temperature at Kalamata (southern Greece) was 40 °C, and at Aydin (western Turkey) it was 41.6 °C. There was a significantly high climatological anomaly (ref: 1979–2009) relating to temperature at 850 hPa over Greece and Turkey from May 12 to May 20. The aim of this study was to evaluate how well this extreme event can be predicted at subseasonal timescales, since it is not a well-researched scientific topic by weather forecasters in the Eastern Mediterranean. Global forecasts from six meteorological centers (ECMWF, UKMO, NCEP, CMA, KMA, HMCR) and WRF simulations produced via CFS (NCEP) analyses and forecasts were examined for lead times ranging from 2 to 6 weeks ahead. The results show that skillful forecasts started 2.5 weeks before the event's onset.

**Keywords:** subseasonal-to-seasonal weather forecasting; S2S; heat wave; maximum air temperature; extreme events; predictability skill



**Citation:** Mitropoulos, D.; Pytharoulis, I.; Zanis, P.; Anagnostopoulou, C. Subseasonal-to-Seasonal Predictability Assessment of an Early Heat Wave in the Eastern Mediterranean in May 2020. *Environ. Sci. Proc.* **2023**, *26*, 42. <https://doi.org/10.3390/environsciproc2023026042>

Academic Editors: Konstantinos Moustiris and Panagiotis Nastos

Published: 24 August 2023



**Copyright:** © 2023 by the authors. Licensee MDPI, Basel, Switzerland. This article is an open access article distributed under the terms and conditions of the Creative Commons Attribution (CC BY) license (<https://creativecommons.org/licenses/by/4.0/>).

## 1. Introduction

Intense and prolonged heat is the leading cause of weather-related deaths worldwide. Heat waves form when high barometric pressure on the surface strengthens and remains over a region for several days to weeks, usually accompanied by the advection of warm air in the lower troposphere. In the context of global warming, a change in heat waves in terms of severity, frequency, and duration is expected. Therefore, it is relevant to explore the ability of the current models to predict heat waves beyond 2 weeks in advance in a subseasonal timescale, giving the state sufficient time to prepare and for mitigation strategies to be implemented.

In recent decades, there have been multiple leaps forward in weather prediction with the help of continuous advances in computing power, weather modeling development and better understanding of the atmospheric processes. However, the predictability horizon seems to have reached an apparent plateau for extreme weather events such as synoptic systems, including heat waves and cold spells. Additionally, climate change seems to influence the occurrence of heat waves in terms of increased frequency, intensity, and duration, leading to rising human morbidity rates and discomfort. On the other hand, in the last decade, some progress has been made in subseasonal forecasting [1] and in the sources of predictability at these timescales [2]. Also, further improvements in numerical weather prediction (NWP) may allow for the existence of predictability beyond 2 weeks. Finally, the demand from users around the world for subseasonal forecasts and the recent international efforts relating to forecasting at this timescale (i.e., 15–45 days lead time) have attracted more attention from scientists with regard to further research on more skillful

forecasts and ultimately establishing the connection between weather forecasting and climate prediction—in other words, seamless prediction.

The aims of this study are as follows: (a) to perform synoptic analysis of the heat wave that occurred on 13–20 May 2020 and (b) to perform predictability assessment of the event for forecasts provided by various meteorological centers and Weather Research and Forecasting Model (WRF) simulations for subseasonal-to-seasonal (S2S) timescales.

## 2. Materials and Methods

### 2.1. Data

The data used are summarized in Table 1. The WRF simulations were produced using the analyses and forecasts of the Climate Forecast System version 2 (CFSv2) from the National Centers for Environmental Prediction (NCEP). This dataset was selected because it provides all the required meteorological fields (i.e., air temperature, dew point, geopotential heights, winds, etc.) across multiple vertical levels to the stratopause (1 hPa) and, most importantly, the forecast window of this dataset covers an adequate time-range of lateral boundary data for the S2S forecasts. The data are provided by NCEP every 6 h with a spatial resolution of  $1^\circ \times 1^\circ$ .

**Table 1.** Data used for parts of the study and their characteristics.

	Name	Centers	Spatial Resolution	Temporal Resolution
<b>WRF Simulations</b>	CFSv2	NCEP	25 km	3 h
<b>Existing S2S Forecasts</b>	S2S Database	ECMWF, NCEP, UKMO, CMA, KMA, HMCR	1.5°	Mondays and Thursdays or Daily (00UTC)
<b>Reanalysis</b>	ERA5 and ERA5-Land	ECMWF	0.25° 0.1°	Hourly
<b>Climatic Parameters</b>	E-OBS and Weather Stations	ECA&D, NOAA and NCDC	0.1° (E-OBS) and Pinpoint Observations	Daily

ECMWF: European Centre for Medium-Range Weather Forecasts; NCEP: National Oceanic and Atmospheric Administration; UKMO: United Kingdom Meteorological Office; CMA: Chinese Meteorological Agency; KMA: Korean Meteorological Agency; HMCR: Hydrometcenter of Russia.

Furthermore, for the predictability estimation of the simulation forecasts, the S2S Prediction Project Database [3] was used (s2s.ecmwf.int and s2s.cma.cn, accessed on 1 March 2021), which provides S2S forecasts from various meteorological centers globally. The real-time data are provided twice per week, daily or weekly (depending on the provider center), with a spatial resolution of  $1.5^\circ \times 1.5^\circ$ .

The analysis was based on datasets of reanalysis data, gridded observations, and observations of weather stations from major Greek cities. The reanalysis data were obtained from the ERA5 Copernicus Climate Change Service database (ECMWF—climate.copernicus.eu, accessed on 15 February 2021). ERA5’s spatial resolution is  $0.25^\circ \times 0.25^\circ$ , and the gridded data are provided hourly across multiple vertical levels to 1 hPa pressure level (37 pressure levels in total). The gridded observations refer to the E-OBS, which is a daily gridded land-only observational dataset over Europe from the station network of the European Climate Assessment & Dataset (ECA&D) project (ecad.eu, accessed on 10 March 2021). This dataset has a spatial resolution of  $0.1^\circ \times 0.1^\circ$  with daily surface variables such as maximum air temperature. The E-OBS surface dataset was also used because of its higher spatial resolution and smaller errors compared to ERA5, in order to produce 95th percentiles of maximum daily air temperature. The weather station observations were obtained from the National Observatory of Athens (NOA) and the database of the National Climatic Data Center of the National Oceanic and Atmospheric Administration (NOAA) ([ncdc.noaa.gov](https://www.ncdc.noaa.gov), accessed on 15 February 2021). In total, 48 weather stations, including numerous stations in Greece and the surrounding countries, were taken into consideration.

## 2.2. Methodology

### 2.2.1. WRF Simulations

In this study, WRF simulations were performed using CFS version 2 (CFSv2) data as initial conditions and boundary conditions, and through dynamical downscaling WRF predictions were performed at a 25 km × 25 km domain. The selected main parameterization schemes are the Thompson graupel (microphysics), Grell–Freitas (cumulus convection), RRTMG (radiation), Mellor–Yamada–Janjic (planetary boundary layer) and Noah (land-surface physics) schemes with 53 vertical levels up to 2 hPa. Sixty simulations were performed with initialization dates from 1 April to 30 April 2020 every 12 h (00 UTC and 12 UTC) and a 3 h temporal resolution of the output. Their lead times spanned from 31 to 61 days according to the initialization date.

### 2.2.2. Excess Heat Factor

The excess heat factor (EHF) [4] was incorporated using two factors (Equation (1)). The first factor (Excessive Heat Index of significance—EHI<sub>sig</sub>) is a measure of how warm a three-day period is with respect to a climatic threshold (such as T<sub>max</sub> 95th percentile) at each location. The second factor (Excessive Heat Index of acclimatization—EHI<sub>accl</sub>) is a measure of how warm the same three-day period is relative to the previous 30-day period, in order to consider the acclimatization to some extent to the local weather conditions.

$$\text{EHF} = \text{EHI}_{\text{sig}} \times \max(1, \text{EHI}_{\text{accl}}), \quad (1)$$

Three consecutive days of EHF > 0 °C<sup>2</sup> is indicative of the presence of a heat wave. In this study, maximum daily air temperatures were used for the calculation of EHF as recommended by previous studies [5].

### 2.2.3. Predictability Scores

The skill assessment of the existing S2S forecasts and the WRF predictions was conducted with the use of relative operating characteristic (ROC) curves. ROC curves in numerical weather prediction quantify forecast quality, mapping the hit rate (HR) against the false alarm rate (FAR). They enable a distinction between skillful forecasts and random chance, improving reliability. By illustrating a model's performance across all thresholds, they facilitate optimal prediction threshold selection. Their insights guide improvements, leading to more accurate, reliable weather forecasts.

In order to construct the ROC curves, a contingency table was needed. The threshold that defined whether a forecast is successful or not was the percentage of ensemble members that successfully forecast the temperature at 850 hPa above its 95th percentile (T<sub>95</sub>) climatological value. The thresholds ranged from 17% to 100% in 6 steps.

The comparison of forecasts and observations (ERA5 reanalysis) was performed for each grid cell and each day (from 8 May to 23 May) for the region of the southern Balkans and western Turkey. The gridcell-to-gridcell comparison is the most rigorous method without any spatial and temporal averages, and it was selected in order to avoid any falsely high predictability skill. The overall comparison of the models was conducted with the area under curve (AUC) measurement which identified a model as skillful when its AUC score was closer to 1. Models with an AUC less than or equal to 0.5 have no predictability skill.

## 3. Results

### 3.1. Synoptic Analysis

The early heat wave for various major cities in Greece (Athens, Thessaloniki, Heraklion, Larisa, and Patra) according to EHF, based on E-OBS, started at different dates (from 11 to 13 May), but the end of the event occurred simultaneously on 20 May with the passing of a cold front. The heat wave for the area of Thessaloniki, according to EHF (E-OBS), started on 13 May and ended on the 20th, lasting 8 days (Figure 1). According to Nairn et al. [4], it is categorized as a heat wave because the EHF was above zero for at least 3 consecutive

days. The EHF based on ERA5 data locates the start of the heat wave on 16 May and the end on the 19th (duration: 4 days). In comparison with the E-OBS, ERA5 shows the peak of the heat wave to be weaker by  $30\text{ }^{\circ}\text{C}^2$  (Figure 1) and to occur a day later (17th May). This difference is mainly due to the different spatial resolutions of the two datasets and their different production methodologies, as E-OBS consists of gridded observations and ERA5 is a reanalysis dataset.

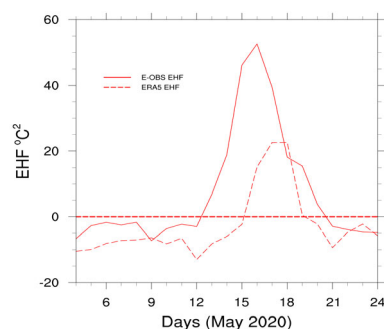


**Figure 1.** EHF ( $^{\circ}\text{C}^2$ ) from E-OBS and ERA5 data for Thessaloniki from 4 to 24 May 2020.

As mentioned previously, the peak of the heat wave is found at different dates, but the most robust results are provided by EHF with the E-OBS data. EHF (E-OBS) identifies the peak intensity as being on 16th May, which agrees with the maximum air temperatures measured from the weather stations of the National Observatory of Athens (NOA) and the Hellenic National Meteorological Service (HNMS) across Greece and the surrounding countries (not shown). This day includes the highest maximum air temperatures recorded in Greece during the heat wave. The highest temperature ( $40\text{ }^{\circ}\text{C}$ ) was recorded in Kalamata, and it was approximately  $17\text{ }^{\circ}\text{C}$  above the 95th percentile of the maximum air temperature value for the specific date. The highest temperature ( $41.7\text{ }^{\circ}\text{C}$ ) in the whole region was recorded in Aydin, Turkey. Additionally, all stations exceeded their  $T_{95\text{max}}$  by  $4\text{ }^{\circ}\text{C}$  to  $17\text{ }^{\circ}\text{C}$  for the 16th of May. Possible reasons for this strong heating are the prolonged low soil moisture accompanied by a blocking high-pressure system. Additionally, a wedge of warm air coming from the Sahara Desert raised the temperature of the lower troposphere and the position of the jet stream northwest of Greece resulted in downward atmospheric movement that led to the amplification of the warming due to thermal compression of the air.

According to the synoptic systems in the vicinity of Greece, at the beginning of the heat wave in the region of Greece, there were stable conditions, with the sea level pressure being approximately 1013 hPa, no fronts were apparent, and surface winds were calm, coming from the SSW and SW. At the end of the heat wave, a cold front approached from the west, bringing cold air masses and lowering the mean daily air temperature across the Eastern Mediterranean. Again, the end of the heat wave fits accordingly to EHF index with the E-OBS data.

The extreme temperatures are also prominent at the lower troposphere. As shown in Figure 2, at an 850 hPa level, the ERA5 data indicate air temperatures higher by 10 standard deviations, or  $14\text{ }^{\circ}\text{C}$  higher than the climatological value above the Aegean Sea. The main reason for the severe warming is the strong thermal advection (maximum value:  $1.5\text{ }^{\circ}\text{C}/\text{h}$ —Western Greece and Albania, not shown) from the southwest for the duration of the event, especially in the western part of Greece. The source of the warm air masses is southeastern Algeria and southwestern Libya, while their path extends north and northeast, affecting southern Italy, Greece and western Turkey.

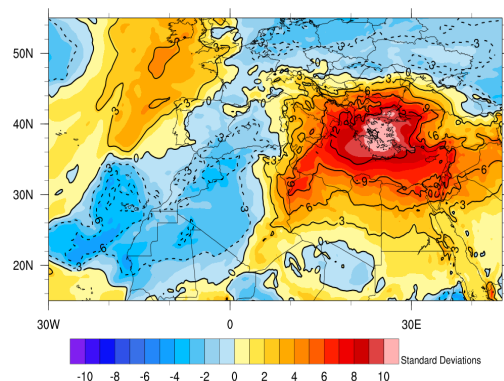


**Figure 2.** Fraction of the ERA5 air temperature anomaly at 850 hPa (relative to the climatology of 1979–2009) to the standard deviation of 16 May 2020 at 12 UTC.

### 3.2. Predictability

This study assesses the 850 hPa air temperature forecasts of the global models of ECMWF, UKMO, NCEP, CMA, KMA, and HMCR, as well as the regional WRF predictions produced using CFSv2 data (NCEP) for the period of 8–23 May 2020. The predictability skill of each model is tested for its initializations from 23 to 29 April 2020. In Figure 3, the ROC curves of all forecasts are presented. It appears that most models present a minor ability to forecast the heat wave, with no exceptional performances. Two of the models (UKMO and HMCR) present no skill, as they are very close to the no-skill line (dashed black line).

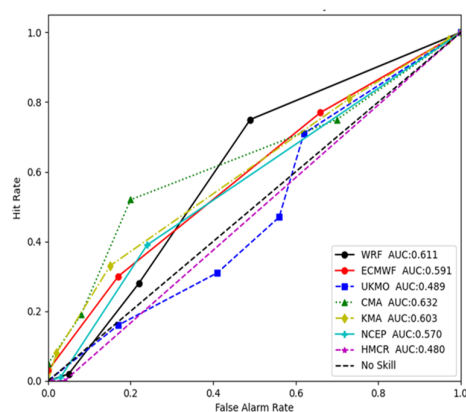


**Figure 3.** ROC curves of six S2S forecasts from the S2S database and the WRF forecasts downscaling the NCEP forecasts to 25 km × 25 km. The probability threshold (points in diagram) ranges from 17% to 100%. The initialization dates are 23–29 April, and the forecast period is 8–23 May. Ensemble members for each model: WRF (14), ECMWF (100), UKMO (21), CMA (6), KMA (21), NCEP (105) and HMCR (19).

The three models (from the S2S database) with the highest skill in this case are CMA, KMA and ECMWF. This is quantitatively justified by their AUC scores (Figure 3), which are all above 0.59. The WRF simulations, which include 14 ensemble members for the period of 23–29 April, show relatively high skill scores compared to the six previously mentioned models, with the second highest AUC score.

The comparison between the NCEP model and the WRF model is more robust since WRF uses NCEP data (CFSv2) as the initial and boundary conditions for its simulations. The AUC score of NCEP is 0.57, while the WRF AUC score is 0.61, which shows that the dynamical downscaling to a spatial resolution of 25 km × 25 km yields more skillful predictions of extreme temperatures at 850 hPa at subseasonal timescales. Furthermore, the hit rate for a probability threshold of 17% is twice as high in WRF (HR = 0.75) than in NCEP

(HR = 0.37). It is noted from Figure 3 that the skill of NCEP with a forecasting probability of 17% has the same approximate skill as WRF with a probability of 33%. This means that WRF shows higher predictability skill than NCEP due to its higher spatiotemporal resolution and its different parameterization schemes that have been selected.

#### 4. Conclusions

The heat wave in this study took place in the region of Greece and western Turkey on May 13 to 20 of 2020 according to the EHF index. The maximum air temperatures recorded were 40 °C in Kalamata (Greece) and 41.6 °C in Aydin (Turkey). The predictability skills of the six models of the S2S database indicate that the heat wave of May 2020 can be predicted even 3 to 4 weeks ahead. WRF, which uses the same initial conditions as NCEP, showed a greater skill score than NCEP due to fact that the simulations were performed at higher spatiotemporal resolutions and can be calibrated (many parameterization schemes) for predicting heat waves. It is expected to have even better skill in predicting the air temperature at the surface because of the complex terrain and land–sea variations of the southern Balkans and eastern Turkey. Finally, dynamical downscaling for small areas such as Greece yields extra forecasting skill regarding heat waves using the WRF model. For this reason, new research is planned for assessing the predictability skill of air temperatures near to the surface, as well the EHF index.

**Author Contributions:** Conceptualization, D.M. and I.P.; methodology, D.M. and I.P.; software, D.M.; validation, I.P., P.Z. and C.A.; formal analysis, D.M.; investigation, D.M.; resources, D.M. and I.P.; data curation, D.M. and I.P.; writing—original draft preparation, D.M.; writing—review and editing, D.M., I.P., P.Z. and C.A.; visualization, D.M.; supervision, I.P.; project administration, D.M. and I.P.; funding acquisition, D.M. All authors have read and agreed to the published version of the manuscript.

**Funding:** The research work was supported by the Hellenic Foundation for Research and Innovation (HFRI) under the 3rd Call for HFRI PhD Fellowships (Fellowship Number: 5413).

**Institutional Review Board Statement:** Not applicable.

**Informed Consent Statement:** Not applicable.

**Data Availability Statement:** The data presented in this study are available upon request from the corresponding author.

**Conflicts of Interest:** The authors declare no conflict of interest.

#### References

1. Ford, T.W.; Dirmeyer, P.A.; Benson, D.O. Evaluation of Heat Wave Forecasts Seamlessly across Subseasonal Timescales. *Npj Clim. Atmos. Sci.* **2018**, *1*, 20. [[CrossRef](#)]
2. Vitart, F.; Robertson, A.W. The Sub-Seasonal to Seasonal Prediction Project (S2S) and the Prediction of Extreme Events. *Npj Clim. Atmos. Sci.* **2018**, *1*, 1–7. [[CrossRef](#)]
3. Vitart, F.; Ardilouze, C.; Bonet, A.; Brookshaw, A.; Chen, M.; Codorean, C.; Déqué, M.; Ferranti, L.; Fucile, E.; Fuentes, M.; et al. The Subseasonal to Seasonal (S2S) Prediction Project Database. *Bull. Am. Meteorol. Soc.* **2017**, *98*, 163–173. [[CrossRef](#)]
4. Nairn, J.R.; Fawcett, R.J.B. The Excess Heat Factor: A Metric for Heatwave Intensity and Its Use in Classifying Heatwave Severity. *Int. J. Environ. Res. Public Health* **2015**, *12*, 227–253. [[CrossRef](#)] [[PubMed](#)]
5. Kueh, M.-T.; Lin, C.-Y. The 2018 Summer Heatwaves over Northwestern Europe and Its Extended-Range Prediction. *Sci. Rep.* **2020**, *10*, 19283. [[CrossRef](#)] [[PubMed](#)]

**Disclaimer/Publisher's Note:** The statements, opinions and data contained in all publications are solely those of the individual author(s) and contributor(s) and not of MDPI and/or the editor(s). MDPI and/or the editor(s) disclaim responsibility for any injury to people or property resulting from any ideas, methods, instructions or products referred to in the content.